nature neuroscience

In utero exposure to cocaine delays postnatal synaptic maturation of glutamatergic transmission in the VTA

Camilla Bellone[1], Manuel Mameli[1,3] & Christian Lüscher[1,2]

Maternal exposure to cocaine may perturb fetal development and affect synaptic maturation in the offspring. However, the molecular mechanism underlying such changes remains elusive. We focused on the postnatal maturation of glutamatergic transmission onto ventral tegmental area dopamine neurons in the mouse. We found that, during the first postnatal week, transmission was dominated by calcium-permeable AMPA receptors and GluN2B-containing NMDA receptors. Subsequently, mGluR1 receptors drove synaptic insertion of calcium-impermeable AMPA receptors and GluN2A-containing NMDAR. When pregnant mice were exposed to cocaine, this glutamate receptor switch was delayed in offspring as a result of a direct effect of cocaine on the fetal dopamine transporter and impaired mGluR1 function. Finally, positive modulation of mGluR1 *in vivo* was sufficient to rescue maturation. These data identify the molecular target through which *in utero* cocaine delays postnatal synaptic maturation, reveal the underlying expression mechanism of this impairment and propose a potential rescue strategy.

About 5% of pregnant women abuse drugs, including cocaine[1]. This affects the health of the mother, which indirectly compromises the well-being of the offspring. In addition, drugs of abuse can have direct effects on the fetus. Cocaine, for example, readily crosses the placenta and the fetal blood-brain barrier, and it has been suggested that this alters fetal development. These alterations manifest as childhood disorders years later[2]. In fact, epidemiological studies associate cocaine exposure *in utero* with enhanced impulsivity, decreased executive function, developmental delays, attention deficit hyperactivity disorder and learning disabilities[3,4]. However, because of confounding factors such as low socio-economic status and abuse of other drugs, a comprehensive meta-analysis failed to identify a distinct syndrome associated with *in utero* cocaine exposure[5].

In utero exposure to cocaine in rodents has previously served as an animal model for the human condition. Several studies using a variety of species and protocols concluded that *in utero* cocaine treatment enhances the subsequent locomotor response to the drug[6,7], increases its self-administration[8–10] and perturbs spatial memory[11]. However, whether working memory and environmental association tasks are affected is less clear[12–14]. Although these studies assessed the behavioral consequences of *in utero* cocaine exposure, they did not reveal the underlying cellular and synaptic mechanisms. For example, the molecular target of cocaine that is responsible for its effects in offspring remains elusive. Cocaine is an alkaloid that inhibits monoamine transporters and blocks ion channels[15]. Given that dopamine (DA) is important for embryonic development[16] and that behavioral disorders triggered by *in utero* cocaine could be caused by altered DA function[2], we focused on the effects of cocaine on the dopamine transporter (DAT) and the development of excitatory transmission in the mesolimbic dopamine system.

In rodents, the ontogeny of the mesolimbic system starts with the aggregation of DA neurons around embryonic day 11 (E11), and the first projections are established 2 d later[17]. The DAT is then expressed on DA neurons at E13 and becomes functional during E15, when DA secretion begins. The topographical specificity of mesostriatal and mesolimbic projections observed in adult mice is established during late embryonic and early postnatal development by the selective elimination of ventral tegmental area (VTA) and substantia nigra pars compacta axon collaterals innervating the dorsal and ventral striatum, respectively[18]. During this time, the basis for regulatory excitatory transmission onto DA neurons is established by the arrival of axons from the prefrontal cortex and several brainstem nuclei. However, when these glutamatergic synapses become functional has not been investigated.

We characterized postnatal synaptic maturation of excitatory transmission onto DA neurons of the VTA and tested the effects of cocaine *in utero* (E11 to E18, that is, until 2 d before delivery) on the offspring. The maturation of glutamatergic synaptic transmission relied on the activation of metabotropic glutamate receptors (mGluR1). Subsequently, we found that cocaine delayed normal maturation via the inhibition of DAT located in DA neurons of the fetus. Finally, *in utero* cocaine affected the potency of mGluR1 on DA neurons and a pharmacological amplification of mGluR1 function in the offspring rescued the cocaine-induced synaptic impairments.

RESULTS

Postnatal maturation of AMPARs and NMDARs

To characterize the postnatal maturation of excitatory synapses onto DA neurons in the VTA, we recorded pharmacologically isolated AMPAR-mediated excitatory postsynaptic currents (EPSCs) in slices

[1]Department of Basic Neurosciences, Medical Faculty, University of Geneva, Geneva, Switzerland. [2]Clinic of Neurology, Department of Clinical Neurosciences, Geneva University Hospital, Geneva, Switzerland. [3]Present address: Institut du Fer à Moulin, Paris, France. Correspondence should be addressed to C.B. (camilla.bellone@unige.ch) or C.L. (christian.luscher@unige.ch).

Received 21 June; accepted 9 August; published online 2 October 2011; doi:10.1038/nn.2930

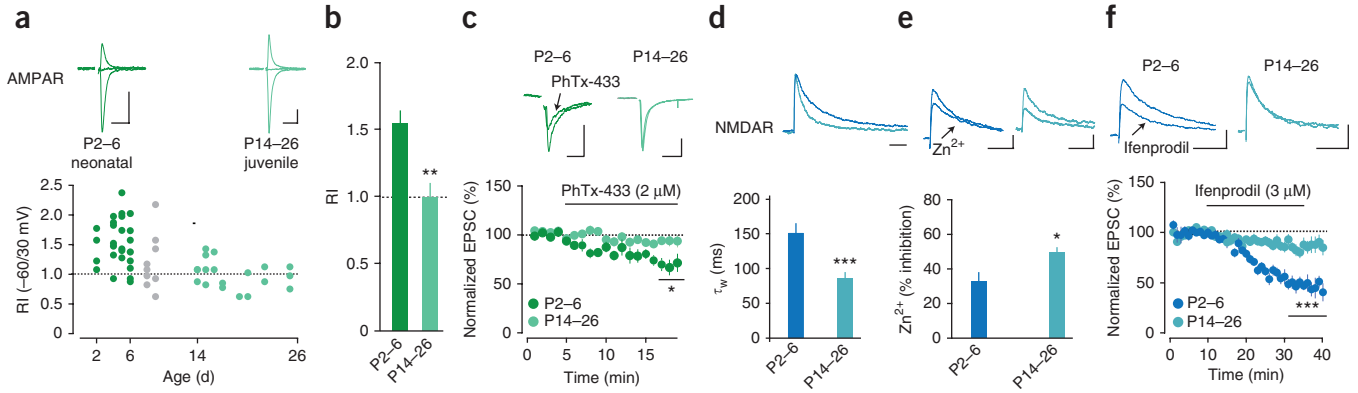

Figure 1 Developmental expression of glutamate receptors in DA neurons. (**a**) Plot of rectification index (RI) as function of postnatal day. Above, averaged example traces of AMPAR-EPSCs recorded at −60, 0 and +30 mV. Scale bars represent 50 pA and 10 ms. Dark green, P2–6; light green, P14–26. (**b**) Bar graph for group data of rectification index (P2–6, 1.55 ± 0.09, $n = 26$; P14–26, 1.0 ± 0.1, $n = 8$; $t_{32} = 3$, $P = 0.0047$). (**c**) Amplitude versus time plot and average example traces of AMPAR-EPSCs in slices at P2–6 and P14–26 in the presence of 2 μM PhTx-433 (inhibition: P2–6, 38.0 ± 7.8%, $n = 5$; P14–26, 8.0 ± 5.3%, $n = 6$; $t_9 = 2.7$, $P = 0.024$). Scale bars represent 50 pA and 10 ms. (**d**) Scaled example traces and decay time for NMDAR-EPSCs (τ_w: P2–6, 151 ± 14 ms, $n = 15$; P14–26, 88 ± 8 ms, $n = 14$; $t_{27} = 3.9$, $P = 0.0005$). Scale bar represents 50 ms. (**e**) Sample traces and effects of Zn^{2+} (300 nM) on NMDAR-EPSCs recorded at +40 mV (Zn^{2+} inhibition: P2–6, 33.3 ± 4.9%, $n = 7$; P14–26, 50.0 ± 2.9%, $n = 5$; $t_{10} = 2.6$, $P = 0.028$). Scale bars represent 100 pA and 50 ms. (**f**) Amplitude versus time plot and sample traces on NMDAR-EPSCs recorded at +40 mV in slices at P2–6 and P14–26 in the presence of 3 μM ifenprodil (P2–6, 48.1 ± 1.5%, $n = 11$; P14–26, 86.3 ± 1.1%, $n = 11$; $t_{20} = 20$, $P < 0.0001$). Scale bars represent 100 pA and 50 ms. Error bars represent s.e.m. $^*P < 0.05$, $^{**}P < 0.01$, $^{***}P < 0.001$.

obtained from mice during the first month of life (**Fig. 1a**). Using the voltage-clamp technique, we measured the EPSC amplitudes at −60, 0 and +30 mV. The younger the mice, the more the amplitudes were disproportionally smaller at positive than at negative potentials. To confirm this inward rectification, we calculated the rectification index as the slope of the line between the current at negative potentials and reversal (that is, the chord conductance) divided by the corresponding slope at positive potentials. The rectification index was substantially higher in postnatal day 2–6 (P2–6) mice than in P14–26 mice, where rectification index had a value of about 1, reflecting linearity (**Fig. 1a**,**b**). We chose these age groups because they correspond to the neonatal and juvenile periods in the mouse life. The high rectification index at P2–6 suggests the presence of GluA2-lacking, calcium-permeable AMPA receptors (CP-AMPARs) in this age group. Confirming this, we observed that the addition of philanthotoxin (PhTx-433), an AMPAR antagonist that is selective for GluA2-lacking receptors, led to a significant reduction of the EPSC amplitude in slices from P2–6 mice ($P < 0.05$), but left transmission in P14–26 slices unaffected (**Fig. 1c** and **Supplementary Fig. 1**). The amplitude of spontaneous EPSCs did not change during maturation, suggesting that the loss of CP-AMPARs is in part compensated by a larger pool of calcium-impermeable AMPA receptors (CI-AMPARs) or simply by more synaptic contacts (**Supplementary Fig. 2**).

At several synapses, a developmental subunit switch from GluN2B- to GluN2A-containing NMDARs has been described[19–21]. We pharmacologically isolated NMDAR-EPSCs at +40 mV in the presence of the $GABA_AR$ antagonist picrotoxin (PTX) and the AMPAR antagonist 2,3-dioxo-6-nitro-1,2,3,4-tetrahydrobenzo[f]quinoxaline-7-sulfonamide disodium salt (NBQX) and determined the relative contribution of these subunits to excitatory transmission onto DA neurons by calculating the decay time kinetics (weighted tau, τ_w) and the pharmacological sensitivity to subtype selective antagonists. We found a slower decay time at neonatal synapses and faster decay at juvenile synapses, an indication of the rearrangement in subunits composition and as would be expected during maturation (**Fig. 1d**). Zn^{2+} (300 nM), a GluN2A antagonist[22], produced a more robust effect at P14–26 than at P2–6 (**Fig. 1e**). This observation was mirrored by the inhibition of EPSCs by ifenprodil (a GluN2B antagonist) in slices from P2–6 mice; this antagonist had a negligible effect in older slices (**Fig. 1f**). Taken together, our data indicate that, during early postnatal development, excitatory synapses onto DA neurons contain a substantial fraction of CP-AMPARs and GluN2B-containing NMDARs, which are replaced with CI-AMPARs and GluN2A-containing receptors by P14.

To confirm the calcium permeability of the AMPARs at neonatal synapses, we filled cells with Oregon green BAPTA-1 and imaged the synaptic entry of calcium while electrically recording synaptic currents. In these recordings, neither DL(−)-2-amino-5-phosphonovaleric acid (DL-AP5) nor Mg^{2+} were added to the superfusion solution to allow NMDAR activation at −60 mV. We identified synaptic hotspots where extracellular stimulation led to robust calcium transients (**Fig. 2a–d**). In slices from P2–6 mice, such transients were unaffected by the NMDAR antagonist DL-AP5, but were virtually abolished by bath application of PhTx-433 for 15 min (**Fig. 2c**,**e**). Conversely, in slices from P14–26 mice, calcium transients were unaffected by PhTx-433, but were completely abolished by DL-AP5 (**Fig. 2d**,**e**). In the presence of DL-AP5 and the voltage-gated calcium channel (VGCC) blockers mibefradil (50 μM) and nimodipine (100 μM), the calcium transient remained unaffected in P2–6 mice (**Fig. 2f**). This confirms that CP-AMPARs contribute to synaptic calcium influx at neonatal synapses.

mGluR1 activation drives maturation of glutamatergic synapses

We next attempted to identify the mechanism that drives the postnatal maturation of glutamatergic synapses onto DA neurons of the VTA. Previously, we characterized a form of mGluR1-mediated synaptic plasticity at these synapses that is expressed by the internalization of GluA2-lacking AMPARs and their replacement by GluA2-containing AMPARs[23,24]. We hypothesized that the activation of mGluR1 receptors could control the postnatal synaptic maturation of both AMPARs and NMDARs at VTA synapses.

If our hypothesis is correct, mice lacking mGluR1s should therefore maintain GluA2-lacking AMPARs and GluN2B-containing NMDARs beyond P6. Our previous findings[24,25] indicate that the induction of mGluR long-term depression (LTD) by DHPG is mediated by mGluR1. We tested our hypothesis in *mGluR1*$^{-/-}$ (also known as *Grm1*) mice[26].

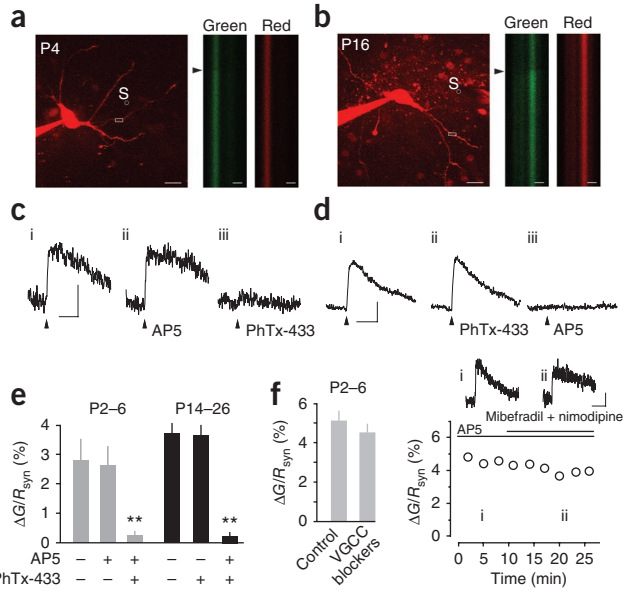

Figure 2 AMPA receptors in DA neurons mediate calcium influx during postnatal development. (**a**) Left, image of a DA neuron at P4. White box represents the line-scan position. Scale bar represents 20 µm. Right, green (Oregon Green BAPTA-1, 100 µM) and red (Alexa FluoRed 594) fluorescence collected in line-scan mode during electrical stimulation at synaptic hotspots (S) (black arrowhead). Scale bars represent 1 µm. (**b**) Similar experiments at P16. Data are presented as in **a**. (**c**) Synaptic Ca^{2+} transients shown as $\Delta G/R$ fluorescence from the same cell as in **a** during baseline (i), in the presence of DL-AP5 (ii) and in the presence of PhTx-433 (iii). Scale bars represent 1% for $\Delta G/R$ and 1 s. (**d**) Synaptic Ca^{2+} transients shown as $\Delta G/R$ fluorescence from the same cell as in **b** during baseline (i), in presence of PhTx-433 (ii) and in presence of DL-AP5 (iii). Scale bars represent 1% for $\Delta G/R$ and 1 s. (**e**) Bar graph indicating group data for $\Delta G/R$ fluorescence in the same conditions as **c** and **d** for P2–6 and P14–26 mice (P2–6: 2.8 ± 0.7 baseline, 2.6 ± 0.6 in AP5 and 0.27 ± 0.01 in PhTx; $F_{2,12} = 6.5$, $P = 0.012$, $n = 5$; P14–26: 3.7 ± 1.2 baseline, 3.71 ± 1.4 in PhTx and 0.16 ± 0.02 in AP5; $F_{2,12} = 5.98$, $P = 0.019$, $n = 5$). $^{**}P < 0.02$. (**f**) Sample traces, timeline and bar graph of synaptically evoked AMPAR-mediated Ca^{2+} transients recorded in presence of AP5 (i) and after application of VGCC blockers (ii) (mibefradil and nimodipine) (5.1 ± 0.5 versus 4.5 ± 0.04; $t_3 = 3.49$, $P = 0.025$, $n = 5$). Error bars represent s.e.m.

We found that AMPARs were rectifying and strongly inhibited by PhTx-433 in slices from P14–26 *mGluR1*$^{-/-}$ mice when compared with slices from wild-type littermates (**Fig. 3a**,**b**). Moreover, NMDAR-EPSCs in *mGluR1*$^{-/-}$ mice showed slower decay kinetics and were strongly sensitive to ifenprodil when compared with wild-type littermates (**Fig. 3c**,**d**). These parameters, measured in interleaved slices from wild-type and knockout mice, were similar to those initially found in control mice (**Fig. 1**). Moreover, neither rectification index nor τ_w differed between wild-type and knockout mice at P2–6, indicating that neonatal synapses were not affected by the absence of mGluR1 (**Fig. 3a**,**c**).

Previously, we found that, in the presence of GluA2-lacking AMPARs, activation of mGluR1 can induce a form of LTD that is expressed by an exchange of GluA2-lacking for GluA2-containing AMPARs[25]. In slices from P2–6 mice, we pharmacologically isolated AMPAR-EPSCs in the presence of PTX and DL-AP5 and recorded EPSCs at −60 mV and +30 mV

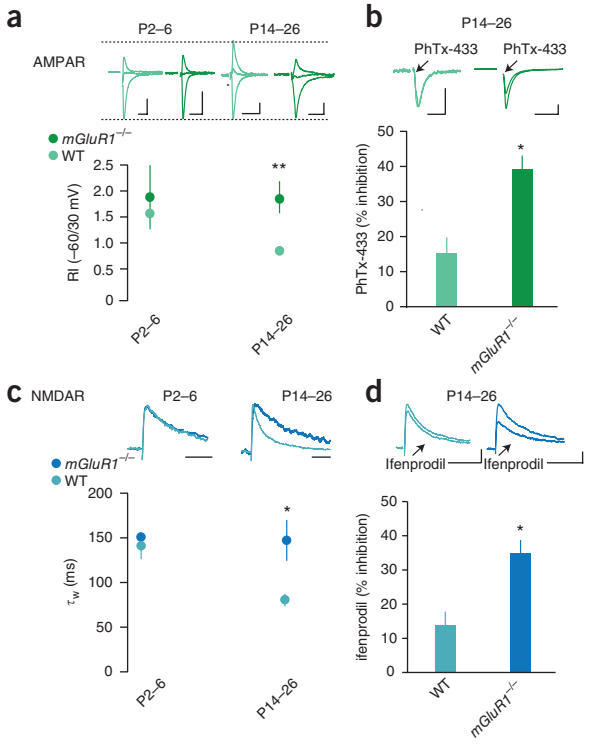

after application of the mGluR1 agonist DHPG (**Fig. 4a**). Although there was a substantial depression of the EPSCs at −60 mV, there was no change at +30 mV (**Supplementary Fig. 3**), indicating a loss of rectification. mGluR1 activation leads to the activation of phospholipase C (PLC) and subsequent release of calcium from internal stores. To determine whether this signaling pathway is involved in driving the insertion of CI-AMPARs, we tested the effect of U73122, an inhibitor of PLC. The DHPG effect was indeed abolished by bath application (**Fig. 4a**). Furthermore, PhTx-433 failed to reduce EPSCs amplitude after addition of DHPG (**Fig. 4b**). Together, these data suggest that CP-AMPARs were replaced by CI-AMPARs via mGluR1 activation and a signaling cascade involving PLC activation.

We next asked whether DHPG had an effect on NMDAR-EPSCs that were pharmacologically isolated at +40 mV in the presence of PTX and NBQX. We found a substantial increase of the amplitude measured at +40 mV, which was blocked by U73122, along with a strong reduction of the ifenprodil sensitivity (**Fig. 4c**,**d**). Consistent with previous reports, these findings suggest that activation of mGluR1s control the synaptic maturation of both AMPARs and NMDARs by inserting GluA2- and GluN2A-containing receptors in a PLC-dependent manner[24,27].

Figure 3 Glutamate receptors maturation in *mGluR1*$^{-/-}$ mice. (**a**) Sample traces of AMPAR-EPSCs (recorded at −60, 0 and +30 mV) and group data for rectification index as a function of postnatal day in wild-type (WT) and *mGluR1*$^{-/-}$ littermate (P2–6: wild type, 1.55 ± 0.1, $n = 5$; *mGluR1*$^{-/-}$, 1.9 ± 0.6, $n = 6$, $P > 0.05$; P14–26: wild type, 0.92 ± 0.07, $n = 7$; *mGluR1*$^{-/-}$, 1.89 ± 0.20, $n = 12$; $t_{17} = 3.02$, $P = 0.008$). Scale bars represent 25 pA and 10 ms. (**b**) Sample traces and effect of PhTx-433 (2 µM) on evoked AMPAR-EPSCs in wild-type and *mGluR1*$^{-/-}$ littermate (wild type, inhibition = 15.3 ± 4.4%, $n = 4$; *mGluR1*$^{-/-}$, 39.4 ± 2.6%, $n = 5$; $t_7 = 4.9$, $P = 0.02$). Scale bars represent 25 pA and 10 ms. (**c**) Scaled sample traces and time course of decay time for NMDAR-EPSCs in wild-type and *mGluR1*$^{-/-}$ littermate at P2–6 and P14–26 (P2–6: wild type, $\tau_w = 150 \pm 6$, $n = 4$; *mGluR1*$^{-/-}$, 138 ± 15, $n = 5$, $P > 0.05$; P14–26: wild type, $\tau_w = 81 \pm 7$, $n = 6$; *mGluR1*$^{-/-}$ 145 ± 31, $n = 6$; $t_{10} = 2$, $P < 0.034$). Scale bars represent 50 pA and 50 ms. (**d**) Sample traces and ifenprodil inhibition of NMDAR-EPSCs in *mGluR1*$^{-/-}$ and wild-type littermates (% of inhibition: *mGluR1*$^{-/-}$, 35.4 ± 3.5%; wild type, 13.6 ± 3.9%; $t_{10} = 4.1$, $P = 0.02$, $n = 5$). Scale bars represent 50 pA and 50 ms. Error bars represent s.e.m. $^{*}P < 0.05$, $^{**}P < 0.01$.

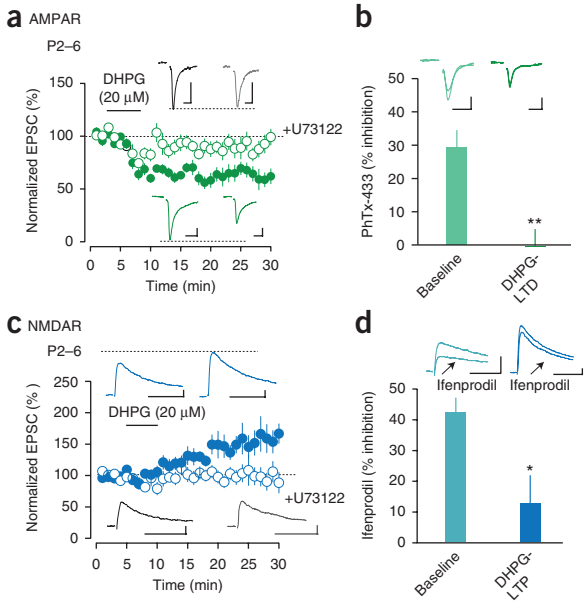

Figure 4 mGluR1s control synaptic maturation of AMPA and NMDA receptors. (**a**) Effect of 5-min application of DHPG on the amplitude versus time plot and sample traces of AMPAR-EPSCs in slices from P2–6 mice recorded at –60 mV in the presence (open circles) or absence (filled circles) of U73122 (5 μM) applied for at least 20 min before recording (filled circles, 61.5 ± 7.0% of baseline, $n = 6$; open circles, 91.1 ± 2.4% of baseline, $n = 5$; $t_{10} = 9$, $P < 0.0001$). Scale bars represent 25 pA and 10 ms. (**b**) Sample traces and PhTx-433 inhibition of AMPAR-EPSCs before and after DHPG application (before DHPG, 29.0 ± 4.8%, $n = 8$; after DHPG, 1.0 ± 4.3%, $n = 5$; $t_{11} = 4.33$, $P = 0.0012$). Scale bars represent 25 pA and 10 ms. (**c**) Effect of DHPG on the amplitude versus time plot and sample traces of NMDAR-EPSCs in slices from P2–6 mice recorded at +40 mV in the presence (open circles) or absence (filled circles) of U73122 (5 μM) applied for at least 20 min (filled circles: 160 ± 20% of baseline, $n = 8$; open circles: 112.6 ± 3.2% of baseline, $n = 5$; $t_{10} = 9$, $P < 0.0001$). Scale bars represent 50 pA and 50 ms. (**d**) Sample traces and ifenprodil inhibition of NMDAR-EPSCs before and after DHPG application at P2–6 (before, 42.5 ± 4.7%, $n = 10$; after, 13.1 ± 9.1%, $n = 6$; $t_{14} = 3.17$, $P = 0.007$). Scale bars represent 50 pA and 50 ms. Error bars represent s.e.m. $^*P < 0.05$, $^{**}P < 0.01$.

Effects of cocaine on synaptic maturation

To test our hypothesis that cocaine can alter postnatal synaptic maturation, we exposed mice to the drug *in utero* and determined the rectification index and sensitivity to PhTx-433 and ifenprodil. To this end, we injected pregnant mice with cocaine (or saline) once a day from E11 until E18. The offspring did not show any notable phenotype. In particular, there was no difference in weight at birth and during subsequent measurements (**Supplementary Fig. 4**). In slices obtained from mice exposed to cocaine *in utero*, a higher rectification index was observed up to P60, but the values dropped back to baseline by P90 (**Fig. 5a**). In addition, pharmacological inhibition of GluA2-lacking AMPARs substantially reduced the EPSC amplitude in cocaine-treated mice at P14–26, but not in those treated with saline (**Fig. 5b**). In contrast with controls, ifenprodil sensitivity remained high and the decay kinetics of NMDA-EPSCs were slow in the *in utero* cocaine-exposed P14–35 mice (**Fig. 5c,d**).

The effects of cocaine seem specific for the synaptic transmission onto DA neurons, as the current-voltage relationships of AMPAR-EPSCs in neighboring GABA VTA neurons were linear in both cocaine- and saline-treated offspring (**Supplementary Fig. 5**). Taken together, our results suggest that daily injections of cocaine from E11 to E18 led to impaired postnatal maturation of glutamatergic transmission onto DA neurons in the VTA.

We attempted to more precisely identify the molecular target responsible for the impairment in synaptic maturation in cocaine-exposed mice. The DAT was proposed as a likely candidate, as it is expressed around the same time as our cocaine treatment (E13). We measured rectification in a knock-in mouse line in which DAT was mutated to become cocaine insensitive (DAT-KI)[28]. We set up

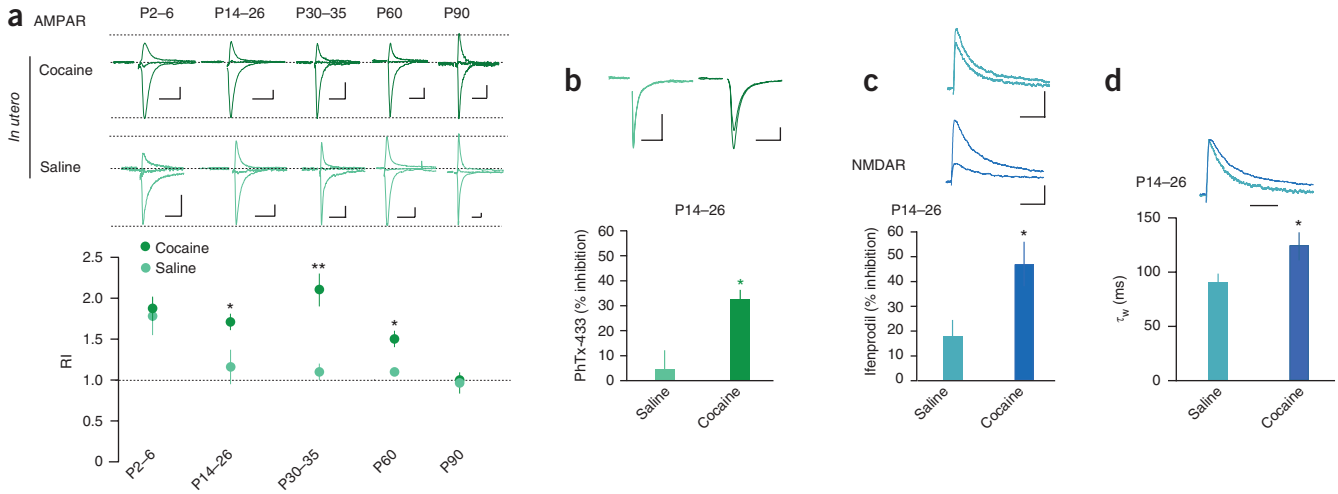

Figure 5 *In utero* cocaine exposure impairs synaptic maturation. (**a**) Top, sample traces of AMPAR-EPSCs (–60, 0 and +30 mV) after cocaine and saline injections *in utero*. Scale bars represent 25 pA and 10 ms. Bottom, rectification index for different age groups after *in utero* cocaine or saline injections (P2–6: cocaine, 1.87 ± 0.15, $n = 12$; saline, 1.78 ± 0.23, $n = 5$; $P > 0.05$; P14–26: cocaine, 1.71 ± 0.10, $n = 17$; saline, 1.16 ± 0.20, $n = 6$; $t_{21} = 2.5$, $P = 0.02$; P30–35: cocaine, 2.1 ± 0.17, $n = 7$; saline, 1.1 ± 0.2; $t_{10} = 4.5$, $P = 0.0012$, $n = 5$; P60: cocaine, 1.50 ± 0.13, $n = 7$; saline, 1.1 ± 0.03, $n = 5$; $t_{10} = 2.6$, $P = 0.02$; P90: cocaine, 0.96 ± 0.13, $n = 6$; saline, 1.03 ± 0.14, $n = 5$; $P > 0.05$). (**b**) Sample traces of AMPAR-EPSCs and bar graph for PhTx-433 inhibition (32.3 ± 3.7% versus 4.9 ± 6.7%, $t_8 = 3.6$, $P = 0.007$, $n = 5$). Scale bars represent 50 pA and 10 ms. (**c**) Sample traces of NMDAR-EPSCs and bar graph for ifenprodil inhibition (saline, 18 ± 5.5, $n = 7$; cocaine, 47 ± 10%, $n = 8$; $t_{13} = 2.4$, $P = 0.03$). Scale bars represent 50 pA and 50 ms. (**d**) Sample traces and decay time for NMDAR-EPSCs (τ_w: cocaine, 127 ± 13, $n = 11$; saline, 91 ± 6, $n = 9$; $t_{18} = 2.2$, $P = 0.04$). Scale bars represent 50 pA and 50 ms. Error bars represent s.e.m. $^*P < 0.05$, $^{**}P < 0.01$.

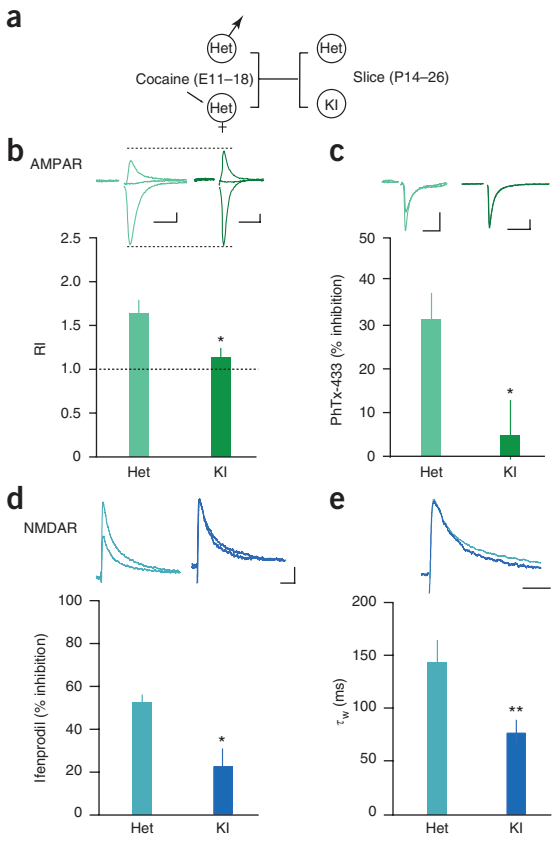

Figure 6 Cocaine-evoked plasticity and postnatal maturation of AMPARs in DAT-KI mice. (**a**) Injection protocol. Heterozygous DAT-KI (Het) male and females were mated and pregnant females injected *in utero* with cocaine once a day (E11–18). Heterozygous and homozygous DAT-KI (KI) offspring were taken for physiology at P14–26. (**b**) Sample traces of AMPAR-EPSCs (–60, 0 and +30 mV) and bar graph of rectification index recorded at P14–26 in heterozygous and homozygous DAT-KI mice born from heterozygous mothers that received cocaine during pregnancy (heterozygous, 1.67 ± 0.17, $n = 6$; homozygous, 1.19 ± 0.09, $n = 9$; $t_{13} = 2.7$, $P = 0.019$). Scale bars represent 25 pA and 10 ms. (**c**) Sample traces and effect of PhTx-433 (2 μM) on evoked AMPAR-EPSCs in heterozygous and DAT-KI offspring (inhibition: heterozygous, 31.5 ± 6.1%, $n = 5$; homozygous, 5.2 ± 8.2%, $n = 7$; $t_{10} = 2.2$, $P = 0.04$). Scale bars represent 25 pA and 10 ms. (**d**) Sample traces and effects of ifenprodil (3 μM) on NMDAR-EPSCs recorded at +40 mV (inhibition: heterozygous, 52.6 ± 2.1%; homozygous, 23.5 ± 11%; $t_8 = 2.6$, $P = 0.03$, $n = 5$). Scale bars represent 100 pA and 50 ms. (**e**) Scaled sample traces and decay time for NMDAR-EPSCs (τ_w: heterozygous, 148 ± 20.3, $n = 9$; homozygous, 79.3 ± 11.7, $n = 7$; $t_{14} = 2.7$, $P = 0.009$). Scale bars represent 50 pA and 50 ms. Error bars represent s.e.m. $^*P < 0.05$, $^{**}P < 0.01$.

heterozygous breeding pairs and compared the rectification index in the offspring at P14–26 (**Fig. 6a**). To ensure that the impaired synaptic maturation was caused by a direct effect of cocaine on the fetus, we first tested whether one injection of cocaine at P14 in DAT-KI mice would elicit the synaptic plasticity of glutamatergic transmission that was previously observed[23,29,30]. To this end, we injected heterozygous and homozygous DAT-KI mice with cocaine, prepared slices a day later and recorded AMPAR-EPSCs. We observed substantial rectification in heterozygous mice, whereas the EPSCs were not affected by cocaine treatment in the homozygous DAT-KI mice (**Supplementary Fig. 6**). We then recorded AMPAR-EPSCs in the offspring of heterozygous DAT-KI dams that had been injected with cocaine during pregnancy (E11–18). The rectification index in P14–26 heterozygous DAT-KI offspring was high (>1.5), whereas the rectification index was close to 1in the homozygous DAT-KI offspring, indicating that AMPAR-EPSCs were linear (**Fig. 6b**). Moreover, PhTx-433 sensitivity was higher in heterozygous DAT-KI offspring (**Fig. 6c**), confirming that the expression of DAT-KI in the fetus was sufficient to prevent impaired synaptic maturation of AMPARs even though the mother remained fully sensitive to cocaine. Similarly, ifenprodil sensitivity was greater and the decay kinetics were slower in heterozygous DAT-KI offspring than in homozygous DAT-KI mice (**Fig. 6d**,**e**). These data indicate that, in wild-type mice, the impairment of synaptic maturation of both AMPARs and NMDARs was caused by a direct effect of cocaine on the DAT in the fetus.

mGluR1 activation rescues *in utero* cocaine impairment

We next asked whether mGluR1 fails to efficiently drive synaptic maturation after *in utero* cocaine treatment. Our data indicate that postnatal maturation of glutamatergic transmission requires mGluR1, but as *in vitro* application of DHPG leads to 'mature' glutamatergic transmission in slices from P2–6 mice, mGluR1 expression and signaling do not represent a limiting factor. Moreover, in P14–26 slices obtained from mice exposed to cocaine *in utero,* DHPG induced a significant depression of AMPAR-EPSCs at –60 mV, which was not the case in slices obtained from mice exposed to saline ($P < 0.001$; **Fig. 7a**). This suggests that prenatal cocaine treatment impairs the synaptic maturation of glutamatergic transmission impeding mGluR1 function, which can be overcome by a saturating concentration of an agonist. To determine whether the difference could be a result of a selective change in potency, we tested the effects of DHPG at a concentration close to its half-maximal effective concentration (EC50)[31]. We found that 10 μM DHPG was enough to elicit mGluR-LTD in slices from P2–6 offspring of saline-injected mothers. Conversely, in the offspring of cocaine-treated dams, this concentration failed to induce LTD (**Fig. 7b**). We reasoned that this decreased sensitivity of mGluR1 receptors could be caused by increased DA levels in the fetal brain when the mother receives the cocaine injections. DA neurons in the VTA express D_2 and D_5 receptors[32,33], and we tested mGluR1 function in the presence of quinpirol and SKF38393, selective D_2-like and D_1-like agonists, respectively. We also monitored transient receptor potential (Trp) channels that were sensitive to the selective antagonist SKF96365 (ref. 34). We found that, while DA receptors were active, DHPG-elicited currents were smaller and had slower kinetics, suggesting a convergence of the signaling cascades of the two receptor systems responsible for Trp channel activation (**Fig. 7c** and **Supplementary Fig. 7**).

We next tested whether positive modulation of mGluR1 *in vivo* could rescue the impaired synaptic maturation after *in utero* cocaine exposure. To this end, we treated P14–26 mice exposed to cocaine *in utero* with a single injection of Ro 67-7476, a positive modulator of mGluR1 (ref. 31), and prepared acute slices 1, 5 or 10 d after injection (**Fig. 8a**). This single injection of Ro 67-7476 was sufficient to restore linear AMPAR-EPSCs in the *in utero* cocaine-treated mice, and this rescue persisted for up to 10 d (**Fig. 8b**). This indicates that boosting mGluR1 function was sufficient to restore the maturation of excitatory transmission and could therefore rescue *in utero* cocaine–induced modification of AMPAR function. As a control, we tested Ro 67-7476 in mice treated with *in utero* saline and observed no effect at any time point. Moreover, a single injection of this positive mGluR1 modulator was able to reduce the ifenprodil inhibition and the NMDAR decay

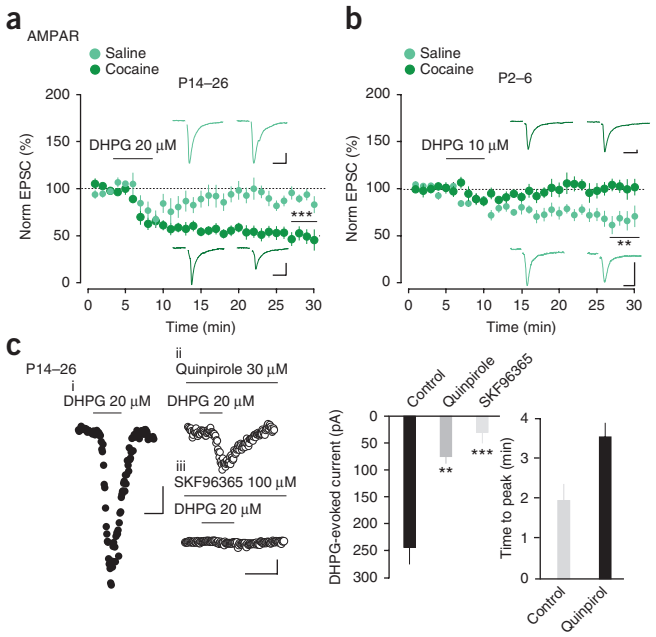

Figure 7 Dopamine modulation of mGluR1. (**a**) Amplitude versus time plots and sample traces of DHPG effect at –60 mV *in utero* cocaine and saline-treated animals (cocaine, 52.8 ± 6.6% of baseline, $n = 6$; saline, 93.6 ± 6.0% of baseline, $n = 7$; $t_{11} = 4.6$, $P = 0.0008$). Scale bars represent 25 pA and 10 ms. (**b**) Amplitude versus time plots and sample traces of DHPG effect on AMPAR-EPSCs recorded at –60 mV *in utero* cocaine and saline offspring (cocaine, 101.9 ± 6.0% of baseline, $n = 8$; saline, 66.4 ± 8.5% of baseline, $n = 7$; $t_{13} = 3.4$, $P = 0.004$). Scale bars represent 25 pA and 10 ms. (**c**) Left, representative traces obtained in DA neurons from wild-type mice showing holding current response to DHPG alone (i), in presence of quinpirole bath-applied for 15 min (ii) or in presence of Trp channel blocker SKF96365 bath-applied for >10 min (iii). Right, change in holding current in the presence of DHPG, DHPG + quinpirole or DHPG + SKF96365 (DHPG, 245 ± 31 pA; DHPG + quinpirole, 76.4 ± 12 pA, $t_8 = 4.97$, $P = 0.001$, $n = 5$; DHPG + SKF96365, 31.3 ± 20 pA, $t_9 = 5.9$, $P = 0.0002$, $n = 6$). The time to peak in the presence of DHPG or DHPG + quinpirole is also plotted (DHPG, 2 ± 0.4; DHPG + quinpirole, 3.6 ± 0.4; $t_7 = 2.7$, $P = 0.03$, $n = 5$). Scale bars represent 50 pA and 3 min. Error bars represent s.e.m. $^{**}P < 0.01$, $^{***}P < 0.001$.

time (**Fig. 8c,d**) in mice treated *in utero* with cocaine. Ro 67-7476 was therefore able to rescue synaptic function of both ionotropic glutamate receptor subtypes.

DISCUSSION

Our results indicate that postnatal maturation of excitatory transmission onto DA neurons of the VTA requires activation of mGluR1. Moreover, we found that cocaine delayed the postnatal maturation of excitatory transmission in mice exposed to the drug between E11 and E18. This second half of gestation in mice corresponds to the second trimester (13–28 weeks) in humans[35], during which cocaine is thought to have a particularly negative effect on the fetus[36]. In mice, this drug-induced impairment affected both AMPAR- and NMDAR-mediated transmission. As a consequence, a substantial fraction of AMPARs in adolescent and young adult mice remained calcium permeable during the first 2 months of life. In parallel, GluN2B-containing NMDARs continued to contribute to EPSCs. We found that DAT expressed on DA neurons in the fetal brain was the *in utero* target of cocaine and was responsible for an excessive increase of DA. Subsequent DA receptor activation then led to long-lasting impaired mGluR1 function. This conclusion is based on the observation that a concentration of DHPG close to EC50 failed to induce LTD at neonatal synapses after cocaine treatment and that positive allosteric modulation of mGluR1 was sufficient to rescue impaired maturation in adolescent mice.

At most CNS synapses, fast and reliable transmission is established only postnatally, in part by molecular rearrangements of the postsynaptic receptors. For example, CP-AMPARs are present in many synapses at birth and are gradually removed during the first weeks of life. CP-AMPARs may confer specific functions to the developing synapse. At mossy fiber–to–CA3 pyramidal neuron synapses, depolarization-induced LTD, present only during early postnatal development, is mediated by CP-AMPARs[37]. Layer 5 neocortical neurons in rats also express CP-AMPARs and switch to CI-AMPARs between P14 and P16 (ref. 38). In addition, GluN2B-containing NMDARs are particularly abundant during the early postnatal period[21].

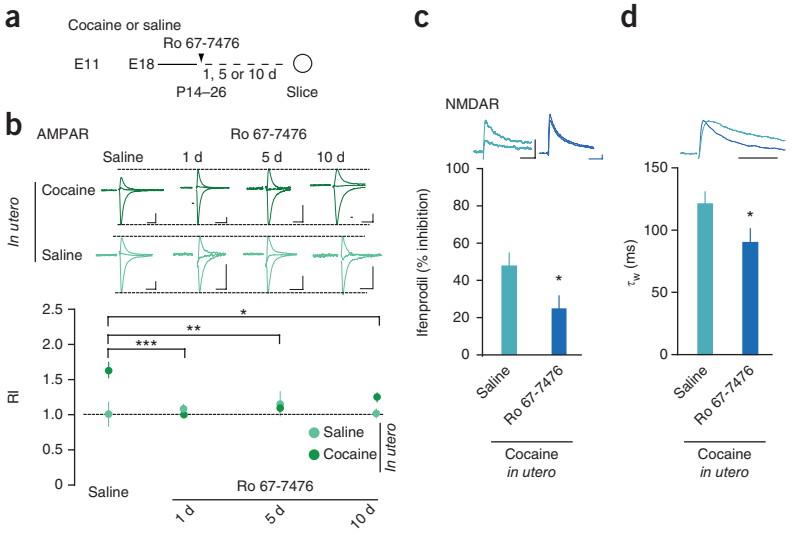

Figure 8 mGluR1 rescues of cocaine-induced impairment of synaptic maturation. (**a**) Injection protocol. Pregnant females were injected once each day with cocaine or saline between E11–18. Offspring were then injected with a single dose of the positive modulator for mGluR1, Ro 67-7476, and killed 1, 5 or 10 d later. (**b**) Sample traces of AMPAR-EPSCs and graph of rectification index recorded 1, 5 and 10 d after a single injection of Ro 67-7476 (4 mg per kg of body weight) in P14–26 mice (cocaine group: 1 d saline, 1.63 ± 0.12, $n = 6$; 1 d Ro 67-7476, 1 ± 0.05, $n = 8$; 5 d Ro 67-7476, 1.1 ± 0.09, $n = 5$; 10 d Ro 67-7476, 1.25 ± 0.08, $n = 8$; $F_{3,23} = 9.3$ $P = 0.0003$, $n = 6$–8; comparison between *in utero* cocaine conditions with Dunnett's multiple comparison test, $P < 0.05$). Scale bars represent 50 pA and 5 ms. (**c**) Sample traces and ifenprodil inhibition of NMDAR-EPSCs after a single injection of saline or Ro 67-7476 24 h before death (ifenprodil inhibition: saline, 47.5 ± 6.8%; Ro 67-7476, 24.8 ± 7%; $t_8 = 2.3$, $P = 0.04$, $n = 5$). Scale bars represent 50 pA and 50 ms. (**d**) Scaled sample traces and decay time for NMDAR-EPSCs (τ_w: saline, 122 ± 8, $n = 6$; Ro 67-7476, 91 ± 11, $n = 9$; $t_{13} = 2$, $P = 0.03$). Scale bars represent 50 pA and 50 ms. Error bars represent s.e.m. $^{*}P < 0.05$, $^{**}P < 0.01$, $^{***}P < 0.001$.

What are the mechanisms that govern the postnatal maturation of glutamatergic receptors? The observations that, in *mGluR1*$^{-/-}$ mice, CP-AMPARs and GluN2B-containing NMDARs remained present much longer after birth suggest that mGluR1 receptors are required for normal postsynaptic maturation in the VTA. Similarly, in excitatory afferents onto stellate cells of the cerebellum, CP-AMPARs remain present until adulthood, but can be removed by strong activity that activates mGluRs[39]. Furthermore, our findings indicate that the signaling pathways that eventually drive the receptor redistribution require PLC, which is consistent with a recent study in the hippocampus and the visual cortex in which the developmental switch from GluN2B to GluN2A was found to be PLC dependent[27]. It is therefore likely that postnatal maturation in the VTA also involves downstream signaling events, such as Ca^{2+} release from IP_3 receptor–dependent stores and PKC activity, even though the receptor that initiates the exchange in the VTA is mGluR1 and not mGluR5, as in the hippocampus and visual cortex[27]. Similar mechanisms may apply to the AMPAR redistribution. In the situation in which CP-AMPARs were observed after cocaine exposure in adult mice[23], mGluR1 activation led to the reinsertion of GluA2-containing receptors in an mTOR- and protein synthesis–dependent manner[24]. Whether the replacement of CP-AMPARs by CI-AMPARs during postnatal development is dependent on protein synthesis will have to be addressed in the future.

What might the repercussions of the prolonged expression of CP-AMPARs and GluN2B-containing NMDARs in the VTA be? Our imaging data indicate that these receptors determine the dendritic calcium source in response to synaptic stimulation. In the first days after birth, a substantial contribution arises from CP-AMPARs in addition to GluN2B-containing NMDAR-mediated calcium transients. Beyond P14, calcium enters the cell through GluN2A-containing NMDARs. Notably, our imaging data suggest that synaptic calcium entry was almost exclusively mediated by CP-AMPARs in P2–6 mice, despite the fact that substantial NMDAR-EPSCs were observed in whole-cell recordings obtained during the same time period. Either the imaging and electrophysiological methods monitored distinct pools of synapses with contrasting properties or these results reflect the presence of NMDARs that are calcium impermeable. In fact, it has been shown that calcium-impermeable GluN3A-containing receptors are preferentially expressed during a narrow temporal window in postnatal development at certain synapses[40]. Given that we found that both the Zn^{2+} and ifenprodil inhibition were partial, the presence of triheteromeric NMDARs (for example, GluN1/GluN2A/GluN2B) at neonatal synapses remains possible. Such noncanonical NMDARs that contain only one GluN2B subunit are less sensitive to ifenprodil[41] than diheteromeric receptors with two GluN2B subunits, which would also explain why inhibition with ifenprodil at P2–6 in the mouse VTA was smaller than has been reported for hippocampus or cortex at this developmental stage[19] or in the rat VTA at P21–29 (ref. 33). Regardless of the precise underlying receptor stoichiometry, the relative change in ifenprodil and Zn^{2+} sensitivity during the first two postnatal weeks is strong evidence for a change in NMDAR subunit composition. Future studies will have to address the consequences of this switch in calcium source for synaptic plasticity[42] and any other process that use synaptic calcium as a second messenger, as these processes ultimately control DA release from these neurons.

The main finding of our study is that *in utero* cocaine exposure delayed postnatal synaptic maturation of DA neurons in the VTA by several months. To identify the molecular target of cocaine, we sought to abolish the pharmacological effect of the drug without interfering with the physiology of the target protein. The DAT-KI mouse, carrying a transporter insensitive to cocaine, but still able to take up endogenous DA[28], was an ideal tool. The observation that cocaine in DAT-KI mice leaves DA neuron firing unaffected demonstrates the efficacy of the point mutations in the DAT[43]. Moreover, DAT-KI mice do not self-administer cocaine and fail to develop conditioned place preference[44,45], which confirms that block of DA reuptake mediates the reinforcing properties of the drug. Although basal DA levels in the DAT-KI mice are slightly higher than normal (64% of baseline), these values are much lower than those seen in the DAT knockout (500% of baseline)[46,47]. In DAT-KI mice, compensatory adaptations are therefore likely to be minimal, which is consistent with our observation that baseline synaptic transmission is normal. Notably, in adult heterozygous DAT-KI mice, cocaine-evoked plasticity in DA neurons was present, whereas synaptic maturation in DAT-KI mice exposed to the drug *in utero* was not impaired. Taken together, these findings represent strong evidence that cocaine initiates its deleterious effect on synaptic maturation at the DAT expressed in the fetal brain.

Our data further indicate that, in the offspring of cocaine-treated mothers, mGluR1s are inefficient in driving postnatal maturation. A likely scenario is that DA concentrations increase because of the DAT inhibition, which activates DA receptors that converge on mGluR1 signaling to reduce their potency. This conclusion is based on the observation that DA receptor agonists reduced mGluR1-evoked Trp currents in the acute slice preparation. Moreover, in slices from mice exposed to cocaine *in utero*, DHPG at a concentration close to EC50 no longer induced the AMPAR redistribution. Thus, our results support previous findings that *in utero* exposure to cocaine leads to sustained increases of DA levels in the striatum[48], which have been reported to cause increased CREB expression[49] and reduced D1 coupling in the nucleus accumbens[50]. Future studies will need to identify the molecular mechanisms that are responsible for the long-lasting nature of the altered potency of mGluR1s. The crucial role of mGluR1 not only indicates the mechanism involved in the impaired maturation, but also suggests a possible treatment. In fact, a positive modulation of mGluR1 was sufficient to trigger maturation and rescue the synaptic alterations caused by *in utero* cocaine exposure.

Finally, our findings also offer a new perspective on cocaine-evoked synaptic plasticity in the VTA of adult mice. One dose of cocaine triggers the appearance of CP-AMPARs and decreases NMDAR function at excitatory synapses onto DA neurons of the VTA[42]. Transmission after a single injection of cocaine strongly resembles transmission during the first week of life. In other words, cocaine may reopen a critical period of postnatal synaptic development. As a consequence of the impairment in synaptic maturation induced by *in utero* cocaine, the window during which calcium can enter the neuron through AMPARs is extended, which may have repercussions for neuronal circuits that are targeted by VTA neurons. The specific synaptic changes onto DA neurons in the VTA may permit more widespread downstream changes. Ultimately, the ensemble of these synaptic adaptations could affect learning and may underlie the behavioral abnormalities observed in children that have been exposed to cocaine during gestation. How delayed synaptic maturation affects behavior and whether boosting mGluR1 signaling represents a potential therapy for children exposed to cocaine *in utero,* remain to be investigated.

METHODS

Methods and any associated references are available in the online version of the paper at http://www.nature.com/natureneuroscience/.

Note: Supplementary information is available on the Nature Neuroscience website.

ACKNOWLEDGMENTS

We thank members of the Lüscher laboratory M. Serafin and A. Holtmaat for critical reading of the manuscript. We thank H.H. Gu, who provided the DAT knock-in mouse line, and K. Huber, who provided the breeding pairs for the mGluR1 mutant mouse line. C.B. is an Ambizione fellow. This work was supported by the Swiss National Science Foundation.

AUTHOR CONTRIBUTIONS

C.B. carried out the *in vitro* electrophysiology experiments with the help of M.M., who performed the imaging experiments. C.L. designed the study and wrote the manuscript with the help of the other authors.

COMPETING FINANCIAL INTERESTS

The authors declare no competing financial interests.

Published online at http://www.nature.com/natureneuroscience/.
Reprints and permissions information is available online at http://www.nature.com/reprints/index.html.

1. Substance Abuse and Mental Health Services Administration. *Results from the 2009 National Survey on Drug Use and Health: Volume I. Summary of National Findings* (Office of Applied Studies, NSDUH Series H-38A, HHS Publication No. SMA 10–4586 Findings) (Rockville, Maryland, 2010).
2. Thompson, B.L., Levitt, P. & Stanwood, G.D. Prenatal exposure to drugs: effects on brain development and implications for policy and education. *Nat. Rev. Neurosci.* **10**, 303–312 (2009).
3. Linares, T.J. *et al.* Mental health outcomes of cocaine-exposed children at 6 years of age. *J. Pediatr. Psychol.* **31**, 85–97 (2006).
4. Mayes, L., Snyder, P.J., Langlois, E. & Hunter, N. Visuospatial working memory in school-aged children exposed *in utero* to cocaine. *Child Neuropsychol.* **13**, 205–218 (2007).
5. Frank, D.A., Augustyn, M., Knight, W.G., Pell, T. & Zuckerman, B. Growth, development, and behavior in early childhood following prenatal cocaine exposure: a systematic review. *J. Am. Med. Assoc.* **285**, 1613–1625 (2001).
6. Crozatier, C. *et al.* Altered cocaine-induced behavioral sensitization in adult mice exposed to cocaine *in utero*. *Brain Res. Dev. Brain Res.* **147**, 97–105 (2003).
7. Hutchings, D.E., Fico, T.A. & Dow-Edwards, D.L. Prenatal cocaine: maternal toxicity, fetal effects and locomotor activity in rat offspring. *Neurotoxicol. Teratol.* **11**, 65–69 (1989).
8. Hecht, G.S., Spear, N.E. & Spear, L.P. Alterations in the reinforcing efficacy of cocaine in adult rats following prenatal exposure to cocaine. *Behav. Neurosci.* **112**, 410–418 (1998).
9. Keller, R.W.J., LeFevre, R., Raucci, J., Carlson, J.N. & Glick, S.D. Enhanced cocaine self-administration in adult rats prenatally exposed to cocaine. *Neurosci. Lett.* **205**, 153–156 (1996).
10. Rocha, B.A., Mead, A.N. & Kosofsky, B.E. Increased vulnerability to self-administer cocaine in mice prenatally exposed to cocaine. *Psychopharmacology (Berl.)* **163**, 221–229 (2002).
11. Trksak, G.H., Glatt, S.J., Mortazavi, F. & Jackson, D. A meta-analysis of animal studies on disruption of spatial navigation by prenatal cocaine exposure. *Neurotoxicol. Teratol.* **29**, 570–577 (2007).
12. Gendle, M.H. *et al.* Prenatal cocaine exposure does not alter working memory in adult rats. *Neurotoxicol. Teratol.* **26**, 319–329 (2004).
13. Thompson, B.L., Levitt, P. & Stanwood, G.D. Prenatal cocaine exposure specifically alters spontaneous alternation behavior. *Behav. Brain Res.* **164**, 107–116 2005).
14. Sobrian, S.K., Ali, S.F., Slikker, W.J. & Holson, R.R. Interactive effects of prenatal cocaine and nicotine exposure on maternal toxicity, postnatal development and behavior in the rat. *Mol. Neurobiol.* **11**, 121–143 (1995).
15. Cantrell, A.R. & Catterall, W.A. Neuromodulation of Na^+ channels: an unexpected form of cellular plasticity. *Nat. Rev. Neurosci.* **2**, 397–407 (2001).
16. Zhou, Q.Y., Quaife, C.J. & Palmiter, R.D. Targeted disruption of the tyrosine hydroxylase gene reveals that catecholamines are required for mouse fetal development. *Nature* **374**, 640–643 (1995).
17. Golden, G.S. Prenatal development of the biogenic amine systems of the mouse brain. *Dev. Biol.* **33**, 300–311 (1973).
18. Hu, Z., Cooper, M., Crockett, D.P. & Zhou, R. Differentiation of the midbrain dopaminergic pathways during mouse development. *J. Comp. Neurol.* **476**, 301–311 (2004).
19. Bellone, C. & Nicoll, R.A. Rapid bidirectional switching of synaptic NMDA receptors. *Neuron* **55**, 779–785 (2007).
20. Monyer, H., Burnashev, N., Laurie, D.J., Sakmann, B. & Seeburg, P.H. Developmental and regional expression in the rat brain and functional properties of four NMDA receptors. *Neuron* **12**, 529–540 (1994).
21. Sheng, M., Cummings, J., Roldan, L.A., Jan, Y.N. & Jan, L.Y. Changing subunit composition of heteromeric NMDA receptors during development of rat cortex. *Nature* **368**, 144–147 (1994).
22. Fayyazuddin, A., Villarroel, A., Le Goff, A., Lerma, J. & Neyton, J. Four residues of the extracellular N-terminal domain of the NR2A subunit control high-affinity Zn^{2+} binding to NMDA receptors. *Neuron* **25**, 683–694 (2000).
23. Bellone, C. & Lüscher, C. Cocaine triggered AMPA receptor redistribution is reversed *in vivo* by mGluR-dependent long-term depression. *Nat. Neurosci.* **9**, 636–641 (2006).
24. Mameli, M., Balland, B., Lujan, R. & Lüscher, C. Rapid synthesis and synaptic insertion of GluR2 for mGluR-LTD in the ventral tegmental area. *Science* **317**, 530–533 (2007).
25. Bellone, C. & Lüscher, C. mGluRs induce a long-term depression in the ventral tegmental area that involves a switch of the subunit composition of AMPA receptors. *Eur. J. Neurosci.* **21**, 1280–1288 (2005).
26. Conquet, F. *et al.* Motor deficit and impairment of synaptic plasticity in mice lacking mGluR1. *Nature* [see comments] **372**, 237–243 (1994).
27. Matta, J.A., Ashby, M.C., Sanz-Clemente, A., Roche, K.W. & Isaac, J.T. mGluR5 and NMDA receptors drive the experience- and activity-dependent NMDA receptor NR2B to NR2A subunit switch. *Neuron* **70**, 339–351 (2011).
28. Chen, R. *et al.* Abolished cocaine reward in mice with a cocaine-insensitive dopamine transporter. *Proc. Natl. Acad. Sci. USA* **103**, 9333–9338 (2006).
29. Argilli, E., Sibley, D.R., Malenka, R.C., England, P.M. & Bonci, A. Mechanism and time course of cocaine-induced long-term potentiation in the ventral tegmental area. *J. Neurosci.* **28**, 9092–9100 (2008).
30. Mameli, M. *et al.* Cocaine-evoked synaptic plasticity: persistence in the VTA triggers adaptations in the NAc. *Nat. Neurosci.* **12**, 1036–1041 (2009).
31. Knoflach, F. *et al.* Positive allosteric modulators of metabotropic glutamate 1 receptor: characterization, mechanism of action, and binding site. *Proc. Natl. Acad. Sci. USA* **98**, 13402–13407 (2001).
32. Khan, Z.U. *et al.* Dopamine D5 receptors of rat and human brain. *Neuroscience* **100**, 689–699 (2000).
33. Schilström, B. *et al.* Cocaine enhances NMDA receptor–mediated currents in ventral tegmental area cells via dopamine D5 receptor–dependent redistribution of NMDA receptors. *J. Neurosci.* **26**, 8549–8558 (2006).
34. Tozzi, A. *et al.* Involvement of transient receptor potential-like channels in responses to mGluR-I activation in midbrain dopamine neurons. *Eur. J. Neurosci.* **18**, 2133–2145 (2003).
35. Clancy, B. *et al.* Web-based method for translating neurodevelopment from laboratory species to humans. *Neuroinformatics* **5**, 79–94 (2007).
36. Stanwood, G.D., Washington, R.A. & Levitt, P. Identification of a sensitive period of prenatal cocaine exposure that alters the development of the anterior cingulate cortex. *Cereb. Cortex* **11**, 430–440 (2001).
37. Ho, M.T. *et al.* Developmental expression of Ca^{2+}-permeable AMPA receptors underlies depolarization-induced long-term depression at mossy fiber CA3 pyramid synapses. *J. Neurosci.* **27**, 11651–11662 (2007).
38. Brill, J. & Huguenard, J.R. Sequential changes in AMPA receptor targeting in the developing neocortical excitatory circuit. *J. Neurosci.* **28**, 13918–13928 (2008).
39. Kelly, L., Farrant, M. & Cull-Candy, S.G. Synaptic mGluR activation drives plasticity of calcium-permeable AMPA receptors. *Nat. Neurosci.* **12**, 593–601 (2009).
40. Roberts, A.C. *et al.* Downregulation of NR3A-containing NMDARs is required for synapse maturation and memory consolidation. *Neuron* **63**, 342–356 (2009).
41. Paoletti, P. & Neyton, J. NMDA receptor subunits: function and pharmacology. *Curr. Opin. Pharmacol.* **7**, 39–47 (2007).
42. Mameli, M., Bellone, C., Brown, M.T. & Lüscher, C. Cocaine inverts rules for synaptic plasticity of glutamate transmission in the ventral tegmental area. *Nat. Neurosci.* **14**, 414–416 (2011).
43. Brown, M.T. *et al.* Drug-driven AMPA receptor redistribution mimicked by selective dopamine neuron stimulation. *PLoS ONE* **5**, e15870 (2010).
44. Thomsen, M., Han, D.D., Gu, H.H. & Caine, S.B. Lack of cocaine self-administration in mice expressing a cocaine-insensitive dopamine transporter. *J. Pharmacol. Exp. Ther.* **331**, 204–211 (2009).
45. Tilley, M.R., O'Neill, B., Han, D.D. & Gu, H.H. Cocaine does not produce reward in absence of dopamine transporter inhibition. *Neuroreport* **20**, 9–12 (2009).
46. Rocha, B.A. *et al.* Cocaine self-administration in dopamine-transporter knockout mice. *Nat. Neurosci.* **1**, 132–137 (1998).
47. Hall, F.S. *et al.* Cocaine-conditioned locomotion in dopamine transporter, norepinephrine transporter and 5-HT transporter knockout mice. *Neuroscience* **162**, 870–880 (2009).
48. Scalzo, F.M., Ali, S.F., Frambes, N.A. & Spear, L.P. Weanling rats exposed prenatally to cocaine exhibit an increase in striatal D2 dopamine binding associated with an increase in ligand affinity. *Pharmacol. Biochem. Behav.* **37**, 371–373 (1990).
49. Guerriero, R.M. *et al.* Augmented constitutive CREB expression in the nucleus accumbens and striatum may contribute to the altered behavioral response to cocaine of adult mice exposed to cocaine *in utero*. *Dev. Neurosci.* **27**, 235–248 (2005).
50. Friedman, E. & Wang, H.Y. Prenatal cocaine exposure alters signal transduction in the brain D1 dopamine receptor system. *Ann. NY Acad. Sci.* **846**, 238–247 (1998).

ONLINE METHODS

Drug treatment. Timed pregnant C57/BL6 mice were housed individually and received daily subcutaneous injections of either cocaine (15 mg per kg of body weight) or saline (0.9% NaCl) between E11 and E18. To minimize skin lesion and tissue necrosis, we rotated the injection sites over different sites on the back. There were no differences in litter size and gender distribution between saline and cocaine groups. The dose of cocaine that we used did not induce seizures or increase mortality.

Electrophysiology in acute brain slices. Horizontal slices from the midbrain (250 μm thick) were prepared following the experimental injection protocols described in the text. Slices were kept in artificial cerebrospinal fluid containing 119 mM NaCl, 2.5 mM KCl, 1.3 mM $MgCl_2$, 2.5 mM $CaCl_2$, 1.0 mM NaH_2PO_4, 26.2 mM $NaHCO_3$ and 11 mM glucose, bubbled with 95% O_2 and 5% CO_2. Whole-cell voltage-clamp recording techniques were used (30–32 °C, 2–3 ml min^{-1}, submerged slices) to measure the holding currents and synaptic responses of DA neurons of the VTA. The VTA is defined as the region medial to the medial terminal nucleus of the accessory optical tract. DA neurons were identified by the presence of a large hyperpolarization-activated (I_h) current immediately after obtaining a whole-cell configuration (80%). The internal solution contained 130 mM CsCl, 4 mM NaCl, 2 mM $MgCl_2$, 1.1 mM EGTA, 5 mM HEPES, 2 mM Na_2ATP, 5 mM sodium creatine phosphate, 0.6 mM Na_3GTP and 0.1 mM spermine. Currents were amplified, filtered at 5 kHz and digitized at 20 kHz. The liquid junction potential was small (−3 mV) and traces were therefore not corrected. In the experiments in which we measured changes in DHPG-induced holding current, the internal pipette solution contained 115 mM potassium methylsulphate, 20 mM NaCl, 1.5 mM $MgCl_2$, 5 mM HEPES, 10 mM BAPTA, 2 mM ATP and 0.3 mM GTP (pH 7.3, 270 mOsm, junction potential of 12 mV). Cells were voltage clamped at −60 mV. All experiments were carried out in the presence of PTX (100 μM); AMPAR EPSCs were pharmacologically isolated by application of the NMDARs antagonist DL-AP5 (100 μM), whereas NMDA EPSCs were pharmacologically isolated by the application of the AMPARs antagonist NBQX (10 μM). The rectification index is the ratio of the chord conductance calculated at negative potential divided by the chord conductance at positive potentials. To simplify the comparison of decay times of NMDARs across conditions, we calculated a single weighted decay measure (referred to in the text as decay time, τ_w) from the area under the peak-normalized current for 1.3 s after the peak. Tricine (*N*-tris(hydroxymethyl)methylglycine, 10 mM) was used to buffer zinc following the relationship $[Zn]_{free} = [Zn]_{added}/200$. The access resistance was monitored by a hyperpolarizing step of −14 mV with each sweep, every 10 s. Experiments were discarded if the access resistance varied by more than 20%. Synaptic currents were evoked by stimuli (0.05–0.1 ms) at 0.1 Hz through bipolar stainless steel electrodes placed rostral to the VTA. Representative example traces are shown as the average of 20 consecutive EPSCs typically obtained at each potential or, in the case of plasticity protocols, during the last 5 min of the baseline and at least 20 min after the induction of plasticity. Compiled data are expressed as mean ± s.e.m. The level of significance was set at $P = 0.05$ as determined by an unpaired *t* test or a one-way ANOVA.

Two-photon microscopy. Dendritic fluorescence was measured with a two-photon laser-scanning microscope based on the Olympus FV-300 system (side-mounted to a BX50WI microscope with a 40×, 0.8 NA, water-immersion objective) and a Mai-Tai laser (Spectra Physics) operating at 810 nm. Green and red fluorescence signals were acquired simultaneously in line-scan mode where the line scan was oriented along the dendrite and quantified as increases in green fluorescence normalized to red fluorescence ($\Delta G/R_{syn}$). Synaptic stimulation was obtained with a glass pipette located proximally to the dendrite. The intracellular solution contained 130 mM cesium-methanesulphonate, 10 mM HEPES, 10 mM sodium phosphocreatine, 4 mM $MgCl_2$, 4 mM Na-ATP, 0.4 mM Na-GTP, 0.1 mM Oregon green BAPTA1 and 0.02 mM AlexaFluo Red. After obtaining the whole-cell configuration, 15–20 min were allowed for intracellular diffusion of fluorophores. Neurons were voltage-clamped at −60 mV to detect a mixture of AMPAR- and NMDAR-mediated responses.

Ethics statement. All the experiments were carried out in accordance with the Institutional Animal Care and Use Committee of the University of Geneva and with permission of the cantonal authorities (Permit No. 1007/3592/2).